

Method for Extraction and Quantification of Metal-Based Nanoparticles in Biological Media: Number-Based Biodistribution and Bioconcentration

Fazel Abdolapur Monikh,^{*,†,‡} Latifeh Chupani,[‡] Eliska Zusková,[‡] Ruud Peters,[§] Marie Vancová,^{||} Martina G. Vijver,[†] Petr Porcal,[⊥] and Willie J.G.M. Peijnenburg^{†,‡,#}

[†]Institute of Environmental Sciences (CML), Leiden University, P.O. Box 9518, 2300 RA Leiden, Netherlands

[‡]South Bohemian Research Centre of Aquaculture and Biodiversity of Hydrocenoses, Faculty of Fisheries and Protection of Waters, University of South Bohemia in České Budějovice, Vodňany, Czech Republic

[§]RIKILT Wageningen UR, Akkermaalsbos 2, 6708 WB Wageningen, Netherlands

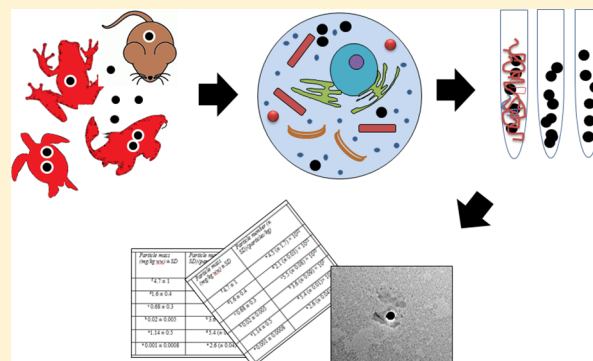
^{||}Biology Centre of the Academy of Sciences of the Czech Republic, Institute of Parasitology, Faculty of Science, University of South Bohemia, Branišovská 31, 37005 České Budějovice, Czech Republic

[⊥]Biology Centre CAS, Institute of Hydrobiology and Soil & Water Research Infrastructure, Faculty of Science, Na Sádkách 7, České Budějovice, Czech Republic

[#]National Institute of Public Health and the Environment (RIVM), Center for Safety of Substances and Products, Bilthoven, Netherlands

S Supporting Information

ABSTRACT: A multistep sample preparation method was developed to separate metal-based engineered nanoparticles (ENPs) from biological samples. The method was developed using spiked zebrafish tissues and standard titanium dioxide (TiO₂) and cerium dioxide (CeO₂) ENPs. Single-particle inductively coupled plasma mass spectrometry was used to quantify the separated particles in terms of number concentration. This method demonstrated mass recoveries of more than 90% and did not strikingly alter the median particles size. High number recoveries were calculated for CeO₂ ENPs (>84%). Particle number recoveries were poor for TiO₂ ENPs (<25%), which could be due to the interference of ⁴⁸Ca with the measured isotope ⁴⁸Ti. The method was verified using zebrafish exposed to CeO₂ ENPs to test its applicability for nanotoxicokinetic investigations. Total mass of Ce and particle number concentration of CeO₂ ENPs were measured in different tissues. Notably, the mass-based biodistribution of Ce in the tissues did not follow the number-based biodistribution of CeO₂. Moreover, the calculated mass-based bioconcentration factors showed a different pattern in comparison to the number-based bioconcentration factors. Our findings suggest that considering mass as the sole dose-metric may not provide sufficient information to investigate toxicity and toxicokinetics of ENPs.



INTRODUCTION

Applying engineered nanoparticles (ENPs) for commercial purposes has raised concerns that these materials may be released into the environment. A growing body of evidence shows that some ENPs are taken up by organisms, distributed in their bodies, and consequently accumulated in various tissues.^{1,2} Most of these studies have been performed by exposing organisms to different mass concentrations of ENPs and assessing the mass-based concentration of the particles accumulated in tissues.³ The toxicokinetics of ENPs, which also are known as nanotoxicokinetics,⁴ cannot be described solely on a mass basis as is the case of classical chemicals.⁵ Unlike chemicals, ENPs have such physicochemical properties

as particle size, number, volume-specific surface area, and composition,⁶ that may affect their toxicokinetics.

However, nanotoxicokinetics remains an under-explored and challenging area. This is mostly due to limitations in characterizing and quantifying ENPs in biological media.⁷ Some techniques have recently been introduced and used to characterize⁸ and quantify⁹ ENPs. Most of these techniques are limited when applied to ENPs in biological media due to the complex and polydisperse matrices encountered there.¹⁰

Received: July 11, 2018

Revised: November 17, 2018

Accepted: December 11, 2018

Published: December 11, 2018

Moreover, the low particle concentrations of ENPs in tissues restrict the direct application of these techniques. Alternatively, a method is required to extract or separate ENPs from biological media in order to decrease the complexity of the media.¹¹ At the heart of the challenge lies the development of a generic sample preparation method capable to separate ENPs from biological matrices while not altering such properties of interest as particle size and number.^{7,12}

Metal-based ENPs cannot be separated from biological samples using the aggressive chemical treatments commonly in use for isolating metal ions (e.g., acid digestion). These approaches lead to dissolution of ENPs and, therefore, substantial alteration in particle size and number. Very recently, Deng et al.¹³ reported that they successfully extracted TiO₂ from plants using an acid digestion approach. The literature offers a few reports on the development of methods for separation of metal-based ENPs from consumer products.^{14–16} Recent studies have presented methodologies to separate and quantify metal-based ENPs in biological samples using alkaline digestion e.g., tetramethylammonium hydroxide (TMAH)^{11,17} and enzymatic digestion.^{17,18} Little attention has been given, however, to optimizing the method to maximize particle recoveries. Particle solubility makes extraction and separation of metal oxide ENPs (e.g., copper oxide [CuO], titanium dioxide [TiO₂], and cerium dioxide [CeO₂]) challenging under the extremely alkaline conditions of, for example, a TMAH solution.¹⁹ Moreover, digestion of tissues to extract and separate ENPs may influence coating agents used on the particles¹² and, consequently, lead to particle aggregation/agglomeration¹¹ and artifacts. Previous studies have been directed to isolating particles from tissues using density gradients and/or direct filtration.¹⁸ These techniques are reported to result in low mass recovery because particles of interest are lost.¹⁹

In this study, we present a generic multistep method for extraction of metal-based ENPs from biological matrices that can be applied for metal and metal oxide ENPs. We must mention that this method was developed for ENPs which do not dissolve or particles with a low dissolution rate. We first optimized and evaluated the method using spiked samples and standard TiO₂ and CeO₂ ENPs. Then, we quantified and characterized the separated ENPs in terms of particle number and median size using single-particle inductively coupled plasma mass spectrometry (sp-ICP-MS) and a transmission electron microscope (TEM). As is often the case in nanotoxicity studies, the low detection levels for number concentration make sp-ICP-MS very promising for the quantification of environmentally relevant particle number concentrations and highly diluted samples.^{20,21} Nevertheless, very few studies have applied this technique for toxicological purposes.^{13,22,17} Finally, the developed method was verified and tested using zebrafish. The separated particles from zebrafish were quantified in terms of particle number concentration and median size to present the number-based biodistribution and number-based bioconcentration factors (NBCFs) of the ENPs in the fish. This study's specific objectives were to (1) develop a generic sample preparation method for extraction and quantification of metal-based ENPs in biological media, and (2) verify that method using exposed zebrafish to test applicability of the method for nanotoxicity investigations and in particular nanotoxicokinetic studies.

■ EXPERIMENTAL SECTION

Reagents and Chemicals. The TiO₂ (NM-104) and CeO₂ (NM-211) ENPs, which are powders, were acquired from the Nanomaterials Repository at the European Commission's Joint Research Centre (JRC).²³ Dispersions of the particles were provided in Milli-Q ultrapure (MQ) water as stock dispersions for different purposes during the study. The dispersions were sonicated before use and only used for a maximum of 24 h. Proteinase K was obtained from Fermentas (Fisher Scientific, Landsmeer, Netherlands). Optima grade hydrochloric acid (HCl, 30%) and nitric acid (HNO₃, 65%) were purchased from Merck (Suprapure, U.S.). Sodium bicarbonate (NaHCO₃), sodium hydroxide (NaOH), sodium dodecyl sulfate (SDS), and hydrogen peroxide (H₂O₂) (30%) were purchased from Sigma-Aldrich (Sigma-Aldrich Corp., St. Louis, MO). Ionic Ti and Ce standards with concentrations of 1000 mg/L were obtained from Merck (Darmstadt, Germany).

We must emphasize that there is no unexpected, new, and/or significant hazards or risks associated with the reported work.

Characterization of TiO₂ and CeO₂ ENPs. An extensive characterization of the physicochemical properties of CeO₂ (NM-211)²⁴ and TiO₂ (NM-104)²⁵ can be found in JRC reports. In this study, TEM images of CeO₂ and TiO₂ dispersions in MQ water were obtained using a JEOL 1010 TEM operated at 70 kV accelerating voltage. About 200 μ L of the dispersion of the particles were pipetted onto copper grids. The grids were kept in darkness at room temperature for 24 h allowing the samples to dry. Hydrodynamic size and zeta potential measurements were made by dynamic light scattering using a Zetasizer Nano device (Malvern Panalytical, Netherlands and UK).

Zebrafish Exposure and Tissue Dissection. Adult zebrafish (*Danio rerio*) were held in the laboratory within the exposure medium for acclimatization. Exposures were conducted in 5 L glass aquariums by introducing a quantity of CeO₂ or TiO₂ ENPs from a 1000 mg/L stock solution to reach final concentrations of 0.5 and 1 mg/L for CeO₂ and TiO₂ ENPs, respectively. The concentrations used in this study were several orders of magnitude higher than those predicted in the environment but still substantially lower than the concentrations reported to be lethal for zebrafish.^{26,27} These concentrations facilitate the measurement of the accumulated particles in the tissues, if accumulation took place. Fish were exposed for 21 days and were fed every 3 days. We replaced the exposure media with fresh media every 36 and 24 h for CeO₂ and TiO₂, respectively. The stock solution was prepared immediately before the exposure test and sonicated using a SONOPULS ultrasonicator (BANDELIN electronic, Berlin, Germany) for 10 min at a delivered power of 40 W. The stability of the particles in the exposure media containing the zebrafish was monitored by measuring the particles concentration, hydrodynamic size over time and TEM measured size. The results were similar to those observed for the media without zebrafish (data not included). After exposure, the intestine, liver, gills, and brain of the fish were immediately dissected and kept frozen for particle extraction. The intestine was divided into three segments including rostral intestinal bulb (RIB), midintestine (MI), and caudal intestine (CI) and were identified in this study as intestine-RIB, intestine-MI, and intestine-CI.

Particle Extraction and Method Optimization. Spike recovery experiments were conducted at 0.1 mg/kg wet weight for CeO₂ and TiO₂ by addition of the ENPs dispersions from stock solution into intestine, liver, gills, and brain samples (presented in this study as spiked tissues). Extraction of CeO₂ and TiO₂ ENPs from tissues consisted of five steps (Figure 1).

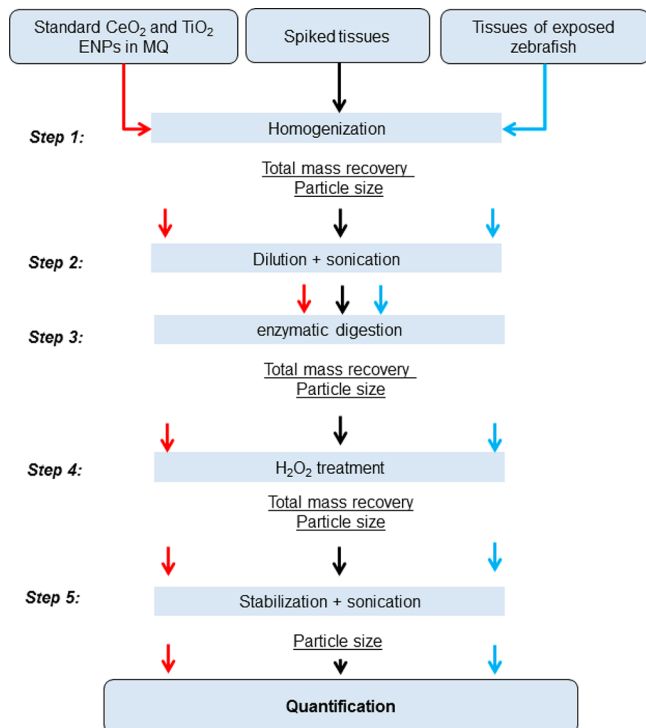


Figure 1. A generic stepwise procedure for developing and evaluating a sample preparation method to separate and quantify metal-based ENPs from biological matrices. The black, red, and blue arrows show the procedure for separating ENPs from spiked tissues, standard CeO₂ and TiO₂ ENPs in MQ water, and tissues of exposed zebrafish, respectively.

Step 1: The fish tissues were homogenized separately using a T 10 basic ULTRA-TURRAX homogenizer (IKA, Staufen, Germany) with a stator diameter of 8 mm, rotor diameter of 6.1 mm, and maximum circumferential speed of 9.6 m/s. To obtain sufficient amounts of sample, tissues of 10 adult zebrafish were homogenized for 1, 5, and 10 min in 1 mL MQ water. **Step 2:** The homogenized tissues were diluted with 1 mL of MQ water and sonicated using a model P30H Elmasonic bath sonicator (Elma Schmidbauer, Singen, Germany) for 10 min to aid in breaking down tissue. **Step 3:** The resulting samples were digested using enzymatic digestion. Accordingly, 5 mL of enzyme solutions (containing 0.05% [w/v] proteinase K, 50 mM ammonium bicarbonate as a buffer, and 0.05% [w/v] SDS) was added to the samples and gently stirred at 50 °C in a water bath. The duration of sample digestion was varied among 2, 10, and 24 h. **Step 4:** Additional post-treatment of the sample was carried out using H₂O₂ at alkaline pH (7.5–8) in a water bath at 90 °C. Temperatures above 65 °C inhibit the activity of proteinase K,²⁸ thus diminishing the possibility of enzyme–H₂O₂ interactions. The duration of sample digestion was 1 h, while the ratio of H₂O₂ to sample was varied among 1:1, 1:2, 1:3, 1:4, and 1:5 (H₂O₂:sample). This process was repeated three times to maximize removal of the biological residuals. **Step 5:** The

obtained suspensions were dispersed using 5 mL of 0.05% SDS solution, followed by sonication for 1, 5, 10, and 20 min at a delivered power of 40 W. We adjusted the pH of the dispersion to 8–8.5 using NaOH.

The total mass recovery (Supporting Information (SI) Formula S1) was calculated to evaluate any losses in the quantity of the particles after each step. Median size was measured after steps 1, 3, 4, and 5 to assess any variation in the median size of the particles during the sample preparation procedures. To achieve the assessment of even minimal alterations of the particle size and number, we evaluated the extraction method using dispersions of standards CeO₂ (NM-211) and TiO₂ (NM-104) ENPs with known primary particle sizes in MQ water. We determined and compared the particle number and median size of the samples before and after particle extraction.

Total Mass Concentration. The samples (tissues and water) were placed into glass tubes and digested for 30–60 min with HNO₃ (65%) at 100–130 °C followed by 2 h of additional digestion with HClO₄ at 170 °C in an aluminum heating block. After digestion, we hydrolyzed the samples with 5 mL of water for 2 h at 100 °C. The total mass concentrations of Ce and Ti in the solutions thus obtained were measured using ICP–MS (Triple Quad 8800, Agilent Technologies). The isotopes ⁴⁷Ti and ¹⁴⁰Ce were measured with a plasma flow of 15.0 L/min and nebulizer gas flow of 1.0 L/min in He mode with integration time of 0.3 s.

Quantification of Median Size and Particles Number Concentration Using sp-ICP–MS. The operational parameters of sp-ICP–MS are summarized in Table 1. Gold (Au)

Table 1. Inductively Coupled Plasma Mass Spectrometry (ICP–MS) Settings for Single Particle Analysis

ICP–MS Parameters	
radio frequency power	1400 W
nebulizer type	conical glass concentric
spray chamber type	quartz impact bead spray
plasma gas flow	13 L/min
nebulizer gas flow	1.1 L/min
auxiliary gas flow	0.7 L/min
isotopes	¹⁴⁰ Ce and ⁴⁸ Ti
Single-Particle ICP–MS Parameters	
dwelt time	3 ms
acquisition time	1 min
replicates per sample	1

ENPs (RM-8013), consisting of a suspension of spherical 60 nm Au ENPs with a mass concentration of 50 mg/L stabilized in a citrate buffer, were obtained from NIST (Boulder, CO) and used as reference materials. A 50 μg/L stock standard was prepared by diluting 50 μL of RM-8013 with 50 mL of MQ water (Millipore A10 system, Millipore, Burlington, MA, USA) and stored at room temperature in amber glass screw-neck vials. Prior to use, the standard was sonicated for 10 min using a bath sonicator. We must mention that in sp-ICP–MS only one isotope can be monitored at a time because of the high time resolution used. Therefore, no internal standards are used. In addition, in sp-ICP–MS a high dilution of the prepared sample suspension is almost always required. As a consequence, matrix effects are limited. Calibration was performed by determining the nebulization efficiency and by

the analysis of ionic analyte standards to determine the mass of individual analyte particles. There are no reference tissues available so far for nanomaterials in general. Therefore, we have applied spiked samples using the standard particles to evaluate the recovery of the extraction method.

Determination of the transport efficiency was carried out according to the method reported by Peters et al.²⁹ Stock standards of Ti and Ce (100 µg/L) were prepared using MQ water. Calibration standards in the concentration range of 0.2–10 µg/L were prepared by diluting the corresponding ionic stock standards further in MQ water. Protected from light, these standards are stable at room temperature for at least 1 week.²⁹

Particle sizes, particle numbers, and mass concentrations were calculated from the results of the instrumental analysis using a single particle calculation tool developed in house (<https://www.wageningenur.nl/en/show/Single-Particle-Calculation-tool.htm>). This tool has been described in detail and validated in previous work.^{29,30}

Data Analysis and Calculation. Data was evaluated statistically for normality using a Kolmogorov–Smirnov test in SPSS version 23.0. One-way analyses of variance (ANOVA) was performed to determine statistically significant differences ($\alpha = 0.05$) between the samples. This was followed by Duncan's post hoc test. Differences between means for two groups were calculated using the *t*-test.

The methods used for calculation of particles size, number concentration and mass concentration using sp-ICP–MS data are described in the Supporting Information. Median size Particle number recoveries were calculated using a formula described in *SI Formula S2*. NBCFs were calculated for each tissue (wet weight) as follows:

$$\text{NBCF(L/kgww)} = \frac{\text{number of particles in tissue (particles/kgww)}}{\text{number of particles in water at 0 h (particles/L)}}$$

RESULTS AND DISCUSSION

Particle Characterization. In this study, the Representative Test Materials (RTMs) CeO₂ (NM-211) and TiO₂ (NM-104) ENPs were used and characterized to support the repository for RTMs launched by the European Commission's JCR. The very low solubility of these particles,^{24,25} moreover, serves to separate particle uptake from the uptake of dissolved particle components. The hydrodynamic size measurements for the particles dispersed in MQ water showed the CeO₂ and TiO₂ to be near those sizes stated by the JRC (*SI Table S1*). The TEM images of the particles (*SI Figure S1*) showed good agreement between the experimentally determined particle size and the reference values reported by JRC (*SI Table S1*) for CeO₂ and TiO₂ ENPs.

Method Development. Evaluation of the Method Using Biological Tissues. One of the challenges in developing a method for separating ENPs from complex matrices lies in the limited availability of representative materials that actually contain the analyte of interest.²⁹ In this study, spiked samples were used as an alternative in the absence of reference materials. It is possible that during sample preparation, a portion of the particles is lost. Moreover, the background matrix (texture of the tissues) where the particles are accumulated may influence the sample preparation method by altering particle size and number. Thus, the extraction process was evaluated using different spiked tissues, including intestine, liver, gills, and brain. The total element mass

recovery and median particle size were the parameters chosen for evaluating each step of the method, whereas homogenization time, digestion times, H₂O₂ concentration, and sonication time were the optimized factors. Optimizing these conditions increases the mass and number recoveries and minimizes the influence of the extraction method on particle size.

The optimal homogenization time was 5 min. After Step 1, the calculated total mass recoveries were between 83% and 113% for Ce and 76% and 107% for Ti. The homogenization step was followed by sonication because the use of sonication is reported to enable more particles to be extracted from their background matrices than is possible without sonication.¹⁹

The optimal enzymatic digestion time of 10 h was chosen for further experiments with all tissues. The total mass recoveries (data mean ± SD) of Ce were 93 ± 5%, 105 ± 9%, 97 ± 3%, and 93 ± 8%, and the total mass recoveries of Ti were 86 ± 8%, 112 ± 9%, 87 ± 5%, and 106 ± 8% for intestine, liver, gills, and brain, respectively. This was at least 5–10% greater than when applying a 2 h enzymatic digestion. A possible explanation for this is that 2 h of digestion is not sufficient for the enzyme solutions to digest large amounts of the tissues and to liberate particles. The particles which remain attached to organic residual in the sample are lost due to adsorption of the organic residual to the tubes during sample preparation and sample handlings.³¹ No significant difference was observed in the total mass recoveries between 10 and 24 h of digestion. The obtained recoveries were higher than those reported in previous studies using enzymatic digestion to separate TiO₂ ENPs^{31,32} and aluminum-containing ENPs¹⁶ from biological samples and consumer products. Our method provided total mass recoveries similar to those reported by Gray et al. for silver (Ag) and Au ENPs in *Daphnia magna* and *Lumbriculus variegatus*.¹⁷

It is possible that after enzymatic digestion biological residues remain in the samples and interfere with particle quantification and characterization³³ (see *SI Figure S2a*). The calculated total mass recoveries after H₂O₂ treatment to remove the organic residual were >91% for Ce and >93% for Ti. Adding H₂O₂ after the enzymatic digestion significantly ($P < 0.05$) improved the CeO₂ particle number recoveries. The ratio of 1:1 was selected as the optimal amount. Although high total mass recoveries were calculated for TiO₂ ENPs after extraction from the spiked samples, we obtained poor number recoveries for these particles. As reported in the literature, it is possible that the selected analytical method, sp-ICP–MS, has limitations in measuring TiO₂ ENPs with sizes smaller than 100 nm.^{34,29} Reed et al. reported that the larger TiO₂ ENPs (~100 nm diameter) yield far fewer pulses above background than do the smaller (~50 to 80 nm diameter) CeO₂ ENPs.³⁵ Another possible explanation is that ⁴⁸Ca of the biological samples interferes with the measured isotope, ⁴⁸Ti, thus causing an elevated background signal. Donovan et al. used ⁴⁷Ti to avoid ⁴⁸Ca interference with ⁴⁸Ti, but the lower abundance of ⁴⁷Ti results in less intense pulses.³⁶

The high number recoveries obtained for CeO₂ can be explained by the fact that H₂O₂ possibly cleaves the bonds between biological residuals and ENPs, which are resistant to enzymatic attack,^{37,28} thus resulting in particles liberation. Particles liberation increases the effectiveness of introducing the sample into the spray chamber of the ICP–MS and consequently greatly improves the particle number recoveries. Combination of H₂O₂ with enzymatic digestion²⁸ and such

Table 2. Total Mass Recoveries, Number Recoveries, And Size of CeO₂ and TiO₂ Engineered Nanoparticles (ENPs) Separated from Spiked Tissues^a

ENP	tissue	total mass recovery (%) mean ± SD	particle number recovery (%) mean ± SD	hydrodynamic size (nm)	median size measured by sp-ICP-MS (nm)	primary particle size (nm) measured by TEM
CeO ₂	intestine	95 ± 5	84 ± 6	275–301	51–57	9–10
	liver	98 ± 2	86 ± 3	229–287	48–56	8–10
	gills	102 ± 5	90 ± 4	215–306	53–58	9–10
	brain	94 ± 4	87 ± 3	256–283	47–58	7–10
TiO ₂	intestine	98 ± 3	<25	293–371	103–310	40–100
	liver	95 ± 1	<25	281–346	136–247	40–100
	gills	93 ± 3	<25	311–357	111–272	60–130
	brain	98 ± 5	<25	248–391	110–237	40–110

^aThe results shown for mass and number recoveries were calculated as means of three independent experiments.

other treatments as tetraacetythylenediamine³⁷ and alkaline wet oxidation³⁸ to remove organic residuals from samples has been tried previously. These studies reported that H₂O₂ at alkaline pH plays an important role in removing biological debris and liberating ENPs.

Particle stability is a prerequisite for further precise measurement of ENPs' size and number concentration.¹⁵ Enzymatic digestion followed by H₂O₂ treatment of tissues may influence particle stability due to removal of coating agents on the particles, thereby making the bare particles prone to aggregation/agglomeration (see SI Figure S2b and d). After H₂O₂ treatment, therefore, we stabilized the separated particles using a 0.05% SDS solution followed by ultrasonication for 1, 5, 10, and 20 min. As reported in the literature, SDS is a suitable dispersant for stabilizing some metal-based ENPs, including TiO₂ ENPs,³⁹ and it is widely used as a dispersant in many industries.⁴⁰ The zeta potential and particle sizes of the stabilized particles, after adjusting the pH (8–8.5) of the dispersion, are reported in SI Table S2. Particle stability was assessed by measuring hydrodynamic particle size changes within 1 h after the stabilization. After 10 and 20 min of ultrasonication, the particle size of both ENPs was stable for 1 h and in good agreement with that obtained for standard CeO₂ and TiO₂ dispersions in MQ water (SI Figure S2c). Less than 10 min of sonication resulted in larger sizes of both particles. Thus, 10 min of sonication was chosen as optimal.

The final results obtained after quantification and characterization for different spiked tissues were compared and are summarized in Table 2. The calculated mass recoveries were between 93% and 102%. No significant difference was observed among the tissues in the total mass recoveries of Ce and Ti. The median size measured by sp-ICP-MS, hydrodynamic size, and TEM-measured particle size were in good agreement with those obtained for standard CeO₂ and TiO₂ dispersions in MQ water. The comparison results also showed there to be no significant difference ($P < 0.05$) between tissues in CeO₂ number recoveries.

Evaluation of the Method Using Standard CeO₂ (NM-211) and TiO₂ (NM-104) in MQ Dispersions. To understand whether the presented sample preparation method influences the particle size and number, we separated TiO₂ (TiO₂ standard NM-104) and CeO₂ (CeO₂ standard NM-211) ENPs from MQ dispersion samples according to the developed method. The calculated total mass recoveries were 98% and 91% for Ce and Ti, respectively (Table 3). The sp-ICP-MS calculated median sizes for the CeO₂ and TiO₂ of 47–57 nm and 148–310 nm, respectively, which is in good agreement

Table 3. Results Obtained for Total Mass Recoveries, Particle Number Recoveries, And Particle Sizes of the Standard CeO₂ and TiO₂ ENPs Dispersed in MQ Water^a

ENP	total mass recovery (%) mean ± SD	particle number recovery (%) mean ± SD	hydrodynamic size (nm)	median size (nm) measured by sp-ICP-MS	primary particles size (nm) measured by TEM
CeO ₂	98 ± 4	91 ± 3	243–281	47–57	8–10
TiO ₂	91 ± 7	<25	289–352	103–310	18–215

^aThe results shown for mass and number recoveries were calculated as means of triplicate extractions.

with the median sizes measured in the same samples prior to particle extraction. The method did not lead to observable alterations in the size of either CeO₂ (<15 nm hydrodynamic size and <5 nm TEM measured primary particle size) or TiO₂ (<3 nm TEM measure primary particle size) ENPs when compared to ENPs analyzed in MQ water prior to extraction.

The particle number recoveries for CeO₂ and TiO₂ were 91% and <25%, respectively. We tested the hypothesis that the low particle number recovery observed for TiO₂ ENPs is related to the limitation of sp-ICP-MS in measuring TiO₂ ENPs and not to the presented extraction method. We measured the particle number of TiO₂ ENPs dispersed in MQ before particles extraction using sp-ICP-MS. The results (data not included) confirmed that the sp-ICP-MS is not able effectively to measure TiO₂ ENPs smaller than ~100 nm, even in the absence of ⁴⁸Ca.

Another issue is that sp-ICP-MS cannot differentiate primary ENPs from aggregated ENPs, and thus the sample preparation method becomes critical.³⁴ To test whether the extraction method influences the particle size (e.g., due to aggregation) and thus the particles number, we observed the separated TiO₂ ENPs using TEM. The results were in good agreement with those obtained for the same ENPs prior to extraction (SI Figure S3).

Performance of the Method. Because spike recovery experiments do not reflect the natural conditions, additional experiments with exposed organisms were conducted to verify and test the method's applicability. Because we did not obtain good particle number recoveries for TiO₂ ENPs, we discuss only CeO₂ ENPs in the following sections.

Mass-Based versus Number-Based Biodistribution. The number-based and mass-based biodistribution of CeO₂ ENPs in the intestine-RIB, intestine-MI, intestine-CI, liver, gills, and brain samples of the zebrafish are summarized in Table 4. Table 4 also shows the measured particle sizes of CeO₂ in

Table 4. Results Obtained for Total Mass of Ce, Particle Number of CeO₂ ENPs, and Median Particle Size of CeO₂ ENPs Accumulated in Tissues of Exposed Zebrafish^a

tissue	particle mass (mg/kg ww) mean ± SD	particle number (mean ± SD) (particles/kg)	hydrodynamic size (nm)	median size measured by sp- ICP-MS (nm)	primary particle size (nm) measured by TEM
intestine-RIB	^f 4.7 ± 1	^e 4.5 (±1.7) × 10 ¹²	242–307	54–55	8–10
intestine-MI	^d 1.6 ± 0.4	^d 2.1 (±0.03) × 10 ¹¹	289–314	50–53	8–10
intestine-CI	^c 0.68 ± 0.3	^c 5.5 (±0.08) × 10 ¹⁰	292–301	47–51	9–10
liver	^b 0.02 ± 0.005	^b 3.6 (±0.09) × 10 ⁵	ND	45–48	8–10
gills	^e 1.14 ± 0.5	^d 5.4 (±0.01) × 10 ¹¹	201–286	48–52	9–10
brain	^a 0.001 ± 0.0008	^a 2.6 (±0.04) × 10 ³	ND	52–57	7–10

^aThe results shown were calculated as means of three independent experiments. ww, wet weight. Different letter superscripts indicate significant differences between tissues ($P < 0.05$); same letter indicates no significant difference ($P > 0.05$). ND, not detected. Concentrations of particles in liver and brain were below the detection limit for the dynamic light scattering method.

tissues. The median size measured by sp-ICP-MS was 45–57 nm, which is in good agreement with the size reported for the CeO₂ dispersion in MQ water. The dynamic light scattering and TEM measured particle sizes for CeO₂ were 201–314 nm and <25 nm, respectively, indicating good agreement with those measured in MQ dispersion and reported by JRC. Statistically significant differences were observed in the total mass of Ce and number concentrations of CeO₂ ENPs between tissues ($p < 0.05$). The mass-based biodistribution of Ce in zebrafish did not follow the number-based biodistribution of CeO₂. Regarding the total mass concentration, there was significant differences between all tissues, with the highest concentration observed in intestine-RIB followed by intestine-MI > gills > intestine-CI > liver > brain. Regarding the particle number concentration, the pattern of CeO₂ accumulation in zebrafish was intestine-RIB > intestine-MI = gills > intestine-CI > liver > brain. There was no significant difference between intestine-MI and gills. The largest number of CeO₂ particles observed in the intestine and in the gills suggests that these tissues are the major end-points of the CeO₂ in this study. This observation could be explained by gastrointestinal uptake or/and a direct contact of the gastrointestinal tract and gills with CeO₂ ENPs in the exposure media as reported in the literature.^{41–43} Our findings also showed that CeO₂ ENPs accumulate in intestine-RIB to a significantly higher level than in intestine-MI and intestine-CI. This observation can be explained by the differences in structure and function of these three sections of intestine.⁴⁴ The presence of CeO₂ ENPs in liver and brain confirmed that these particles are transported to internal organs. According to the TEM- and sp-ICP-MS-measured particles sizes, transport of CeO₂ into internal tissues occurred without any striking shift in median particle size. Geraets et al. had reported that CeO₂ can be distributed to internal tissues other than lung, such as liver, kidney, spleen, brain, and testis, after a single 6 h exposure.⁴⁵

Mass-Based versus Number-Based Bioconcentration Factor. Results for mass-based bioconcentration factors (MBCFs) of Ce and NBCFs of CeO₂ in zebrafish tissues are summarized in Table 5. The MBCFs of Ce in intestine-RIB were higher than those in other tissues and were followed by intestine-MI > gills > intestine-CI. Low MBCFs were calculated for liver (0.05 L/kg) and brain (0.002 L/kg). The NBCFs showed a different pattern in comparison to MBCFs, with the highest level being that for intestine-RIB, followed by the gills. Interestingly, comparing MBCF and NBCF values shows that the MBCFs values are higher in all tissues except for the intestine-RIB. The amount of ionic Ce measured by sp-

Table 5. Calculated MBCFs of Ce and NBCFs of CeO₂ ENPs in Tissues of the Exposed Zebrafish

tissue	MBCFs (L/kg) ± SD	NBCFs (L/kg) ± SD
intestine-RIB	10 ± 0.9	19 ± 0.67
intestine-MI	3 ± 0.3	0.89 ± 0.15
intestine-CI	1 ± 0.16	0.02 ± 0.003
liver	0.05 ± 0.003	1 × 10 ⁻⁶ ± 4 × 10 ⁻⁷
gills	2 ± 0.24	2 ± 0.46
brain	0.002 ± 0.0004	9 × 10 ⁻⁹ ± 9.6 × 10 ⁻¹⁰

ICP-MS was 1.2, 0.4, and 0.2 mg/kg for intestine-RIB, intestine MI and intestine-CI, respectively, whereas it was lower than the detection limits in the liver, brain and gills. Although we have assumed that the CeO₂ particles remain stable throughout the process of applying the method, it is likely that some degree of particle dissolution does occur within cell and tissues. Similar findings have been reported from previous studies, suggesting that a small fraction of CeO₂ taken up by plants undergoes dissolution despite particle stability in the exposure media.^{46,47} This leads to a decrease in the number of particles within tissues and can explain the differences observed between MBCFs and NBCFs in intestine MI and intestine-CI. It is also possible that the size of the particles in the tissues is lower than the detection limit in terms of size of the instrument (30–40 nm) for CeO₂. Smaller particles were thus not detected while still present. Further investigation of this issue is out of the scope of this study and needs to be performed in future studies. As measured by MBCFs, our results show that bioconcentration took place in intestine-RIB, intestine-MI, intestine-CI, and gills. As measured by NBCFs, bioconcentration was observed only in intestine-RIB and gills. This finding suggests that to consider mass as the sole dose-metric does not provide the proper information to investigate nanotoxicokinetics. This is as predicted in the literature,^{48,49} and it is a key finding for future environmental nanotoxicology studies.

■ ASSOCIATED CONTENT

📄 Supporting Information

The Supporting Information is available free of charge on the ACS Publications website at DOI: 10.1021/acs.est.8b03715.

Additional information as noted in the text (PDF)

■ AUTHOR INFORMATION

Corresponding Author

*E-mail: f.a.monikh@cml.leidenuniv.nl.

ORCID 

Fazel Abdolapur Monikh: 0000-0001-9500-5303

Notes

The authors declare no competing financial interest.

ACKNOWLEDGMENTS

We acknowledge the core facility supported by the Czech-BioImaging large RI project (LM2015062 funded by the Ministry of Education, Youth and Sports of the Czech Republic) for its support in obtaining the scientific data. The study was supported by Ministry of Education, Youth, and Sports of the Czech Republic projects CENAKVA (No. CZ.1.05/2.1.00/01.0024), CENAKVA II (No. LO1205 under the NPU I program), LM2015075, and EF16_013/0001782. The research was partially supported by the European Union's Horizon 2020 research and innovation programme under grant agreement number 760813 "PATROLS" and the Grant Agency of the University of South Bohemia (projects nos. 012/2016/Z and 065/2015/Z). We wish to acknowledge the JRC Nanomaterials Repository as supplier of the materials. We also thank J. Willemse (Institute of Biology Leiden University, Leiden, Netherlands), G. van Bommel (RIKILT Wageningen WUR, Netherlands), and M. Tesařová (Institute of Parasitology, University of South Bohemia, Czech Republic) for their considerable technical assistance.

REFERENCES

(1) Jackson, B. P.; Bugge, D.; Ranville, J. F.; Chen, C. Y. Bioavailability, Toxicity, and Bioaccumulation of Quantum Dot Nanoparticles to the Amphipod *Leptocheirus Plumulosus*. *Environ. Sci. Technol.* **2012**, *46* (10), 5550–5556.

(2) Jung, Y.-J.; Kim, K.-T.; Kim, J. Y.; Yang, S.-Y.; Lee, B.-G.; Kim, S. D. Bioconcentration and Distribution of Silver Nanoparticles in Japanese Medaka (*Oryzias Latipes*). *J. Hazard. Mater.* **2014**, *267*, 206–213.

(3) Hao, L.; Chen, L.; Hao, J.; Zhong, N. Bioaccumulation and Sub-Acute Toxicity of Zinc Oxide Nanoparticles in Juvenile Carp (*Cyprinus Carpio*): A Comparative Study with Its Bulk Counterparts. *Ecotoxicol. Environ. Saf.* **2013**, *91*, 52–60.

(4) Confalonieri, U.; Akhtar, R.; Hauengue, M.; Revich, B.; Woodward, A.; Menne, B.; Ebi, K. L.; Kovats, R. S. *Human Health*; 2007. DOI: 10.5822/978-1-61091-484-0_15.

(5) Grass, R. N.; Limbach, L. K.; Athanassiou, E. K.; Stark, W. J. Exposure of Aerosols and Nanoparticle Dispersions to in Vitro Cell Cultures: A Review on the Dose Relevance of Size, Mass, Surface and Concentration. *J. Aerosol Sci.* **2010**, *41* (12), 1123–1142.

(6) Stoeger, T.; Reinhard, C.; Takenaka, S.; Schroepel, A.; Karg, E.; Ritter, B.; Heyder, J.; Schulz, H. Instillation of Six Different Ultrafine Carbon Particles Indicates a Surface Area Threshold Dose for Acute Lung Inflammation in Mice. *Environ. Health Perspect.* **2006**, *114* (3), 328–333.

(7) Handy, R. D.; Von Der Kammer, F.; Lead, J. R.; Hassellöv, M.; Owen, R.; Crane, M. The Ecotoxicology and Chemistry of Manufactured Nanoparticles. *Ecotoxicology* **2008**, *17*, 287–314.

(8) Domingos, R. F.; Baalousha, M. a.; Ju-nam, Y.; Reid, M. M.; Tufenkji, N.; Lead, J. R.; Leppard, G. G.; Wilkinson, K. J. Characterizing Manufactured Nanoparticles in the Environment: Multimethod Determination of Particle Sizes Characterizing Manufactured Nanoparticles in the Environment: Multimethod Determination of Particle Sizes. *Environ. Sci. Technol.* **2009**, *43*, 7277–7284.

(9) Johnson, M. E.; Hanna, S. K.; Bustos, A. R. M.; Petersen, E. J.; Bryant, C.; Yu, L. L. Using Single Particle ICP-MS as a Tool for Understanding Metallic Nanoparticle Transformation during Nanotoxicity Assays Single Particle-ICP-MS. **2014**, *3*, 97–100.

(10) von der Kammer, F.; Ferguson, P. L.; Holden, P. A.; Mason, A.; Rogers, K. R.; Klaine, S. J.; Koelmans, A. A.; Horne, N.; Unrine, J. M. Analysis of Engineered Nanomaterials in Complex Matrices (Environment and Biota): General Considerations and Conceptual Case Studies. *Environ. Toxicol. Chem.* **2012**, *31* (1), 32–49.

(11) Johnson, M. E.; Hanna, S. K.; Montoro Bustos, A. R.; Sims, C. M.; Elliott, L. C. C.; Lingayat, A.; Johnston, A. C.; Nikoobakht, B.; Elliott, J. T.; Holbrook, R. D.; Scott, K. C. K.; Murphy, K. E.; Petersen, E. J.; Yu, L. L.; Nelson, B. C. Separation, Sizing, and Quantitation of Engineered Nanoparticles in an Organism Model Using Inductively Coupled Plasma Mass Spectrometry and Image Analysis. *ACS Nano* **2017**, *11* (1), 526–540.

(12) Arslan, Z.; Ates, M.; McDuffy, W.; Agachan, M. S.; Farah, I. O.; Yu, W. W.; Bednar, A. J. Probing Metabolic Stability of CdSe Nanoparticles: Alkaline Extraction of Free Cadmium from Liver and Kidney Samples of Rats Exposed to CdSe Nanoparticles. *J. Hazard. Mater.* **2011**, *192* (1), 192–199.

(13) Deng, Y.; Petersen, E. J.; Challis, K. E.; Rabb, S. A.; Holbrook, R. D.; Ranville, J. F.; Nelson, B. C.; Xing, B. Multiple Method Analysis of TiO₂Nanoparticle Uptake in Rice (*Oryza Sativa* L.) Plants. *Environ. Sci. Technol.* **2017**, *51* (18), 10615–10623.

(14) Lu, P. J.; Huang, S. C.; Chen, Y. P.; Chiueh, L. C.; Shih, D. Y. C. Analysis of Titanium Dioxide and Zinc Oxide Nanoparticles in Cosmetics. *Journal of Food and Drug Analysis* **2015**, *23* (3), 587–594.

(15) Wagner, S.; Legros, S.; Loeschner, K.; Liu, J.; Navratilova, J.; Grombe, R.; Linsinger, T. P. J.; Larsen, E. H.; Von Der Kammer, F.; Hofmann, T. First Steps towards a Generic Sample Preparation Scheme for Inorganic Engineered Nanoparticles in a Complex Matrix for Detection, Characterization, and Quantification by Asymmetric Flow-Field Flow Fractionation Coupled to Multi-Angle Light Scattering And. *J. Anal. At. Spectrom.* **2015**, *30* (6), 1286–1296.

(16) Loeschner, K.; Correia, M.; López Chaves, C.; Rokkjær, I.; Sloth, J. J. Detection and Characterisation of Aluminium-Containing Nanoparticles in Chinese Noodles by Single Particle ICP-MS. *Food Addit. Contam., Part A* **2018**, *35* (1), 86–93.

(17) Gray, E. P.; Coleman, J. G.; Bednar, A. J.; Kennedy, A. J.; Ranville, J. F.; Higgins, C. P. Extraction and Analysis of Silver and Gold Nanoparticles from Biological Tissues Using Single Particle Inductively Coupled Plasma Mass Spectrometry. *Environ. Sci. Technol.* **2013**, *47* (24), 14315–14323.

(18) Jiménez-Lamana, J.; Wojcieszek, J.; Jakubiak, M.; Asztemborska, M.; Szpunar, J. Single Particle ICP-MS Characterization of Platinum Nanoparticles Uptake and Bioaccumulation by: *Lepidium Sativum* and *Sinapis Alba* Plants. *J. Anal. At. Spectrom.* **2016**, *31* (11), 2321–2329.

(19) Schwertfeger, D. M.; Velicogna, J. R.; Jesmer, A. H.; Saatcioglu, S.; McShane, H.; Scroggins, R. P.; Princz, J. I. Extracting Metallic Nanoparticles from Soils for Quantitative Analysis: Method Development Using Engineered Silver Nanoparticles and SP-ICP-MS. *Anal. Chem.* **2017**, *89* (4), 2505–2513.

(20) Mitrano, D. M.; Ranville, J. F.; Bednar, A.; Kazor, K.; Hering, A. S.; Higgins, C. P. Tracking Dissolution of Silver Nanoparticles at Environmentally Relevant Concentrations in Laboratory, Natural, and Processed Waters Using Single Particle ICP-MS (SpICP-MS). *Environ. Sci.: Nano* **2014**, *1* (3), 248–259.

(21) Lee, S.; Bi, X.; Reed, R. B.; Ranville, J. F.; Herckes, P.; Westerhoff, P. Nanoparticle Size Detection Limits by Single Particle ICP-MS for 40 Elements. *Environ. Sci. Technol.* **2014**, *48* (17), 10291–10300.

(22) Coleman, J. G.; Kennedy, A. J.; Bednar, A. J.; Ranville, J. F.; Laird, J. G.; Harmon, A. R.; Hayes, C. A.; Gray, E. P.; Higgins, C. P.; Lotufo, G.; Steevens, J. A. Comparing the Effects of Nanosilver Size and Coating Variations on Bioavailability, Internalization, and Elimination, Using *Lumbricus Variegatus*. *Environ. Toxicol. Chem.* **2013**, *32* (9), 2069–2077.

(23) Cotogno, G.; Totaro, S.; Rasmussen, K.; Pianella, F.; Roncaglia, M.; Olsson, H.; Sintes, J. R. *The JRC Nanomaterials Repository - Safe handling of nanomaterials in the sub-sampling facility*; 2016. DOI: 10.2788/088893.

- (24) Singh, C.; Friedrichs, S.; Ceccone, G.; Gibson, N.; Jensen, K. A.; Levin, M.; Goenaga Infante, H.; Carlander, D.; Rasmussen, K. *Cerium Dioxide, NM-211, NM-212, NM-213: Characterisation and Test Item Preparation*; 2014. DOI: 10.2788/80203.
- (25) Rasmussen, K.; Mast, J.; Temmerman, P.-J. De.; Verleysen, E.; Waegeneers, N.; Steen, F. Van.; Pizzolon, J. C.; Temmerman, L. De.; Doren, E. Van.; Jensen, K. A.; Birkedal, R.; Levin, M.; Nielsen, S. H.; Koponen, I. K.; Clausen, P. A.; Kofoed-Sørensen, V.; Kembouche, Y.; Thieriet, N.; Spalla, O.; Guiot, C.; Rousset, D.; Witschger, O.; Bau, S.; Bianchi, B.; Motzkus, C.; Shivachev, B.; Dimowa, L.; Nikolova, R.; Nihtianova, D.; Tarassov, M.; Petrov, O.; Bakardjieva, S.; Gilliland, D.; Pianella, F.; Ceccone, G.; Spampinato, V.; Cotogno, G.; Gibson, N.; Gaillard, C.; Mech, A. *Titanium Dioxide, NM-100, NM-101, NM-102, NM-103, NM-104, NM-105: Characterisation and Physico-Chemical Properties*, 2014. DOI: 10.2788/79554.
- (26) Chen, J.; Dong, X.; Xin, Y.; Zhao, M. Effects of Titanium Dioxide Nano-Particles on Growth and Some Histological Parameters of Zebrafish (*Danio Rerio*) after a Long-Term Exposure. *Aquat. Toxicol.* **2011**, *101* (3–4), 493–499.
- (27) Wehmas, L. C.; Anders, C.; Chess, J.; Punnoose, A.; Pereira, C. B.; Greenwood, J. A.; Tanguay, R. L. Comparative Metal Oxide Nanoparticle Toxicity Using Embryonic Zebrafish. *Toxicology Reports* **2015**, *2*, 702–715.
- (28) Shen, G.; Tao, H.; Zhao, M.; Yang, B.; Wen, D.; Yuan, Q.; Rao, G. Effect of Hydrogen Peroxide Pretreatment on the Enzymatic Hydrolysis of Cellulose. *J. Food Process Eng.* **2011**, *34* (3), 905–921.
- (29) Peters, R. J. B.; Rivera, Z. H.; Van Bommel, G.; Marvin, H. J. P.; Weigel, S.; Bouwmeester, H. Development and Validation of Single Particle ICP-MS for Sizing and Quantitative Determination of Nano-Silver in Chicken Meat Characterisation of Nanomaterials in Biological Samples. *Anal. Bioanal. Chem.* **2014**, *406* (16), 3875–3885.
- (30) Peters, R.; Herrera-Rivera, Z.; Undas, A.; van der Lee, M.; Marvin, H.; Bouwmeester, H.; Weigel, S. Single Particle ICP-MS Combined with a Data Evaluation Tool as a Routine Technique for the Analysis of Nanoparticles in Complex Matrices. *J. Anal. At. Spectrom.* **2015**, *30* (6), 1274–1285.
- (31) Shaw, B. J.; Ramsden, C. S.; Turner, A.; Handy, R. D. A Simplified Method for Determining Titanium from TiO₂ Nanoparticles in Fish Tissue with a Concomitant Multi-Element Analysis. *Chemosphere* **2013**, *92* (9), 1136–1144.
- (32) Sun, H.; Zhang, X.; Niu, Q.; Chen, Y.; Crittenden, J. C. Enhanced Accumulation of Arsenate in Carp in the Presence of Titanium Dioxide Nanoparticles. *Water, Air, Soil Pollut.* **2007**, *178* (1–4), 245–254.
- (33) Loeschner, K.; Brabrand, M. S. J.; Sloth, J. J.; Larsen, E. H. Use of Alkaline or Enzymatic Sample Pretreatment Prior to Characterization of Gold Nanoparticles in Animal Tissue by Single-Particle ICPMS Characterisation of Nanomaterials in Biological Samples. *Anal. Bioanal. Chem.* **2014**, *406* (16), 3845–3851.
- (34) Aznar, R.; Barahona, F.; Geiss, O.; Ponti, J.; José Luis, T.; Barrero-Moreno, J. Quantification and Size Characterisation of Silver Nanoparticles in Environmental Aqueous Samples and Consumer Products by Single Particle-ICPMS. *Talanta* **2017**, *175*, 200–208.
- (35) Reed, R. B.; Higgins, C. P.; Westerhoff, P.; Tadjiki, S.; Ranville, J. F. Overcoming Challenges in Analysis of Polydisperse Metal-Containing Nanoparticles by Single Particle Inductively Coupled Plasma Mass Spectrometry. *J. Anal. At. Spectrom.* **2012**, *27*, 1093.
- (36) Donovan, A. R.; Adams, C. D.; Ma, Y.; Stephan, C.; Eichholz, T.; Shi, H. Single Particle ICP-MS Characterization of Titanium Dioxide, Silver, and Gold Nanoparticles during Drinking Water Treatment. *Chemosphere* **2016**, *144*, 148–153.
- (37) Sun, R.; Tomkinson, J. Characterization of Hemicelluloses Isolated with Tetraacetylenediamine Activated Peroxide from Ultrasound Irradiated and Alkali Pre-Treated Wheat Straw. *Eur. Polym. J.* **2003**, *39* (4), 751–759.
- (38) Klinke, H. B.; Ahring, B. K.; Schmidt, A. S.; Thomsen, A. B. Characterization of Degradation Products from Alkaline Wet Oxidation of Wheat Straw. *Bioresour. Technol.* **2002**, *82* (1), 15–26.
- (39) López-Heras, I.; Madrid, Y.; Cámara, C. Prospects and Difficulties in TiO₂ Nanoparticles Analysis in Cosmetic and Food Products Using Asymmetrical Flow Field-Flow Fractionation Hyphenated to Inductively Coupled Plasma Mass Spectrometry. *Talanta* **2014**, *124*, 71–78.
- (40) Mafuné, F.; Kohno, J.; Takeda, Y.; Kondow, T.; Sawabe, H. Structure and Stability of Silver Nanoparticles in Aqueous Solution Produced by Laser Ablation. *J. Phys. Chem. B* **2000**, *104* (35), 8333–8337.
- (41) Gaiser, B. K.; Fernandes, T. F.; Jepson, M.; Lead, J. R.; Tyler, C. R.; Stone, V. Assessing Exposure, Uptake and Toxicity of Silver and Cerium Dioxide Nanoparticles from Contaminated Environments. In *Environmental Health: A Global Access Science Source*, 2009; Vol. 8. DOI: 10.1186/1476-069X-8-S1-S2.
- (42) Johnston, B. D.; Scown, T. M.; Moger, J.; Cumberland, S. A.; Baalousha, M.; Linge, K.; Van Aerle, R.; Jarvis, K.; Lead, J. R.; Tyler, C. R. Bioavailability of Nanoscale Metal Oxides TiO₂, CeO₂, and ZnO to Fish. *Environ. Sci. Technol.* **2010**, *44* (3), 1144–1151.
- (43) Gagnon, C.; Bruneau, A.; Turcotte, P.; Pilote, M.; Gagné, F. Nanomedicine & Nanotechnology Fate of Cerium Oxide Nanoparticles in Natural Waters and Immunotoxicity in Exposed Rainbow Trout. *J. Nanomed. Nanotechnol.* **2018**, *9* (2), 2157–7439.
- (44) Wang, Z.; Du, J.; Lam, S. H.; Mathavan, S.; Matsudaira, P.; Gong, Z. Morphological and Molecular Evidence for Functional Organization along the Rostrocaudal Axis of the Adult Zebrafish Intestine. *BMC Genomics* **2010**, *11*, 392.
- (45) Geraets, L.; Oomen, A. G.; Schroeter, J. D.; Coleman, V. A.; Cassee, F. R. Tissue Distribution of Inhaled Micro- and Nano-Sized Cerium Oxide Particles in Rats: Results from a 28-Day Exposure Study. *Toxicol. Sci.* **2012**, *127* (2), 463–473.
- (46) Zhang, P.; Ma, Y.; Zhang, Z.; He, X.; Zhang, J.; Guo, Z.; Tai, R.; Zhao, Y.; Chai, Z. Biotransformation of Ceria Nanoparticles in Cucumber Plants. *ACS Nano* **2012**, *6* (11), 9943–9950.
- (47) Hernandez-Viezcas, J. A.; Castillo-Michel, H.; Andrews, J. C.; Cotte, M.; Rico, C.; Peralta-Videa, J. R.; Ge, Y.; Priester, J. H.; Holden, P. A.; Gardea-Torresdey, J. L. In Situ Synchrotron X-Ray Fluorescence Mapping and Speciation of CeO₂ and ZnO Nanoparticles in Soil Cultivated Soybean (*Glycine Max*). *ACS Nano* **2013**, *7* (2), 1415–1423.
- (48) Oberdörster, G.; Oberdörster, E.; Oberdörster, J. Nanotoxicology: An Emerging Discipline Evolving from Studies of Ultrafine Particles. *Environ. Health Perspect.* **2005**, *113*, 823–839.
- (49) Hua, J.; Vijver, M. G.; Chen, G.; Richardson, M. K.; Peijnenburg, W. J. G. M. Dose Metrics Assessment for Differently Shaped and Sized Metal-Based Nanoparticles. *Environ. Toxicol. Chem.* **2016**, *35* (10), 2466–2473.